Shahrood University of Technology

Journal of Mining and Environment (JME)

Journal homepage: www.jme.shahroodut.ac.ir

Iranian Society of Mining Engineering (IRSME)

Finite Difference Analysis of Empirical Tunnel Support Design in High Stress Fractured Rock Mass Environment at Bunji Hydropower Project, Pakistan

Hafeezur Rehman[1,2], Wahid Ali[1], Kausar Sultan Shah[3], Mohd Hazizan Bin Mohd Hashim[2*], Naseer Muhammad Khan[4], Muhammad Ali[1], Muhammad Kamran[5], and Muhammad Junaid[3]

1. Department of Mining Engineering, Balochistan University of Information Technology Engineering and Management Sciences, Quetta, Pakistan
2. School of Materials and Mineral Resources Engineering, University Sains Malaysia, Engineering Campus, Nibong Tebal, Penang, Malaysia
3. Department of Mining Engineering, Karakoram International University, Gilgit, Pakistan
4. Department of Sustainable Advanced Geomechanical Engineering, Military College of Engineering, National University of Sciences and Technology, Risalpur, Pakistan
5. Department of Mining Engineering, Institute of Technology Bandung, Indonesia

Article Info

Received 22 August 2022

Received in Revised form 29 August 2022

Accepted 2 September 2022

Published online 2 September 2022

DOI:10.22044/jme.2022.12231.2219

Keywords

High in-situ stresses

Tunnel support

Jointed rock mass

Numerical modelling

Empirical methods

Abstract

Support design is the main goal of the Q and rock mass rating (RMR) systems. An assessment of the Q and RMR system application in tunnelling involving high-stress ground conditions shows that the first system is more appropriate due to the stress reduction factor. Recently, these two systems have been empirically modified for designing the excavation support pattern in jointed and highly stressed rock-mass conditions. This research work aims to highlight the significance of the numerical modelling, and numerically evaluate the empirically suggested support design for tunnelling in such an environment. A typical horse-shoe-shaped headrace tunnel at the Bunji hydropower project site is selected for this work. The borehole coring data reveal that amphibolite and Iskere Gneiss are the main rock mass units along the tunnel route. An evaluation of the proposed support based on the modified empirical systems indicate that the modified systems suggest heavy support compared to the original empirical systems. The intact and mass rock properties of the rock units are used as the input for numerical modelling. From numerical modelling, the axial stresses on rock bolts, thrust bending moment of shotcrete, and rock load from modified RMR and Q-systems are compared with the previous studies. The results obtained indicate that the support system designed based on modified version of the empirical systems produce better results in terms of tunnel stability in high-stress fractured rock mass conditions.

1. Introduction

In Pakistan, the design and construction activities along with the policies in the hydropower sector show the government's seriousness to increase the hydropower generation capacity in the country [1]. The northern area of the country is a feasible position for constructing the hydropower projects. Sub-surface excavation is a major component of nearly all hydropower projects in the region due to the existence of Himalaya. In Himalayas, the construction of the underground project is always a challenging task, both technically and financially. The region is tectonically active, geologically young, and also affected by geological structures of varying extents [2]. During underground construction, the geological factors (rock mass properties, groundwater inflow, and virgin stress settings) disturb the stability of the excavation [3-5]. Due to deep excavation practice, the problems like groundwater inflow, rock bursting, and squeezing are faced in almost every project [6]. The complexities associated with the Himalayas make the in-situ environment more challenging for tunnel using tunnel boring machines (TBMs) [2]. Despite these challenges, several tunnels have been

Corresponding author: mohd_hazizan@usm.my (M.H.B. Mohd Hashim).

completed in the last decade in the region. From these completed projects, considerable experiences were gained and replicated in the form of research works. These research activities explored and evaluated the critical role of rock mechanics in the underground structures construction and design. During and after the completion of these projects, the tunnel face mapping, characterization, and the supports pattern are used for the extension of the RMR and Q-systems for the relevant ground [7, 8].

Analysis of the in-situ stress magnitude and orientation, rock mass quality, project-related features, and boundary conditions are vital for tunnel support design and stabilization [4, 5]. In this context, the tunnel excavation methods, excavation sequencing patterns, and corresponding support are based on the complex relations between project cost, safety, and schedule [9]. Precise characterization of rock mass defines the excavation behavior, whereas classification of rock mass predicts the construction cost and safety assessment in tunneling. Empirical classification systems are established on characterization and developed and updated for defining rock mass quality, and used with underground excavation span to determine the preliminary support [10].

Tunnel support design and stability evaluation is the main concern during their design and construction. Empirical systems like RMR, GSI (Geological Strength Index), and Q systems [11-15] are used internationally for the determination of rock quality and the design of tunnel support pattern. Recently, the applications of the two systems (Q and RMR) have been empirically extended to tunnelling in highly stressed fractured rock situations [8, 16, 17]. Although the empirical systems are modified to these conditions for the classification of rock mass and tunnel support pattern determination, these systems cannot provide details about the support performance, stress rearrangement, and rock load determination under different circumstances.

Tunnel modelling in a realistic and precise way to increase the confidence related with rock mass characterization and replicate its intrinsic spatial heterogeneities and variabilities [18]. During this modelling, different modelling techniques like precedent type analysis, experimental testing, analytical methods, empirical classification, basic and extended numerical modelling, and basic and integrated system approaches are used. In engineering application, the researchers use at least two different approaches for project assessment [19-22]. Numerical modelling such as DEM (discrete element method), FEM (finite element method), and FDM (finite difference method) along with BEM (boundary element method) have been used widely in geo-technical projects design and construction [23, 24]. In tunnelling, these modelling packages are used not only in conventional excavation but also appropriate for suitable reinforcement strategies during TBM tunnelling [25]. Ali *et al.* [26] have used FEM 3D modelling for topography induced stress and its influence on tunnel excavation in hard rocks. Nikadat and Marji [27], [28] and Manouchehrian, Marji *et al.* [23] have used BEM and FEM for the stress distribution and displacement analysis around the tunnel. Lee *et al.* [29] and Rehman *et al.* [30] have used FDM analysis to evaluate rock load and tunnel excavation sequence for stability assessment.

In this work, the rock mass along the headrace tunnels of the 7100 MW Bunji Hydropower Project (BHP) is characterized and classified based on the modified versions of RMR and Q from the previous studies. The tunnel support of a typical horse shoe shaped was designed keeping in view the scope of modified versions of the classification systems. Rock mass characterization was carried out based on the exploration data conducted during the project's design stage. Field and laboratory test information was used, and rock mass properties were determined using the Hoek-Brown failure criterion [31]. These information were further used as the input data in FLAC 2D for numerical modelling. Excavation sequence and supports are derived using empirical systems and used in modelling. Through numerical modelling, tunnel stability was evaluated and compared in terms of axial stress on rock bolts, shotcrete stability, and rock load.

2. Project Description and Geology

The proposed BHP is situated in the Gilgit-Baltistan region of Pakistan (shown in Figure 1) [32]. In Pakistan, the project is the largest hydroelectric project in terms of designed capacity (7100 MW). The dam site of the project is about 12 km upstream of Sassi, a nearby town, and about 60 km SE of the Gilgit city. The powerhouse is located some 5 km downstream of the confluence of the Indus and Gilgit Rivers and about 43 km downstream of the proposed dam site. The powerhouse area is near the junction point of the three mountain ranges, Himalaya, Hindukush, and Karakoram. At this location, the Indus River flows

around the Sarkund Ridge, which provides a high potential head for power generation over a short, direct distance.

The project exploration reports reveal that the 11.6 m span and 8-km long headrace tunnels (5 No.s) will be excavated in the fractured rock under high in-situ stresses. These tunnels will convey the 1,900m³/s of design discharge to the powerhouse.

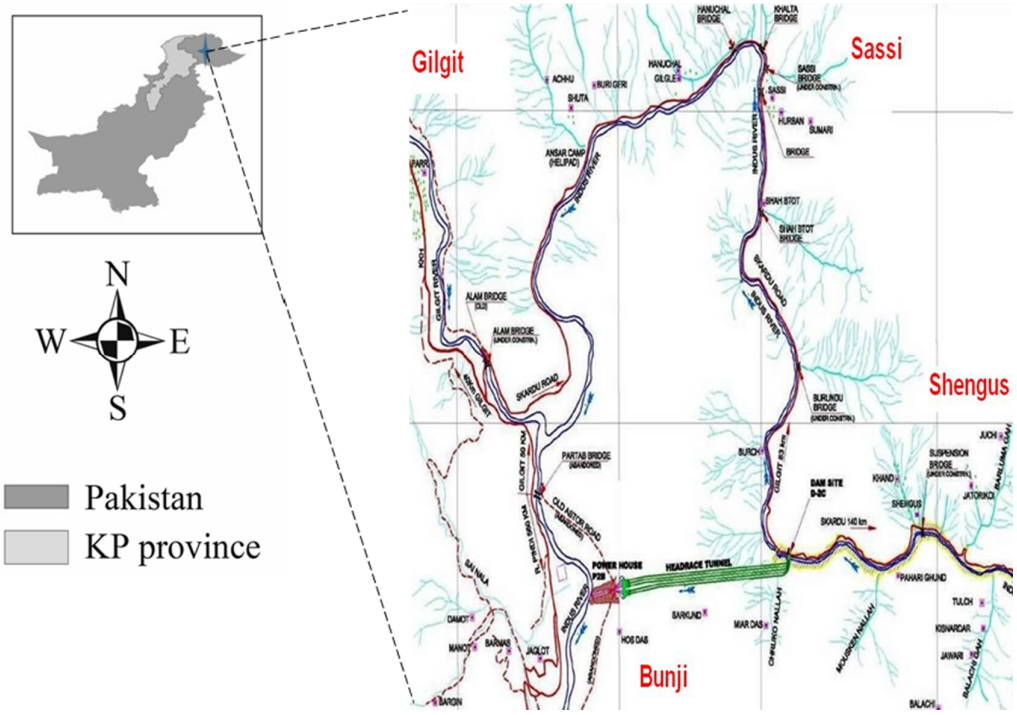

Figure 1. Location of project in Pakistan.

The sub-continent has been surrounded by the Himalayas and the Indian Ocean, the most distinctive geographical structures, and has a common source. They are produced via geodynamic processes including the opening of the Indian Ocean and sea-floor spreading. Due to the forces from geodynamics, the Indian Plate collided with the Eurasian Plate, and as a result, shaped the Himalayas and nearby ranges. This part of the world is, therefore, tectonically active due to plates (Eurasian and Indian) collision. The BHP lies near the boundary of the Eurasian and Indian Plates.

In the Himalayas, microplates and the main lithospheric plates are under movement; subsequently, the height of the Himalayas increases with time. From these movements, the geography is divided into litho-tectonic parts in terms of compressional and extensional faulting [33] including Lesser, Tethyan, and Higher Humalayas along with Trans-Himalaya, Sub-Himalaya, and major bounding faults [34]. Strike-slip faulting is also the main activity within the collision zone periphery. The Main Mantle Thrust (MMT) is a major fault passing through the project area.

3. Field and laboratory studies

In this work, four types of surface and sub-surface investigation methods have been used to explore further the geology and geomorphology of the project area including surface geological mapping, boreholes, exploratory adits, and scanning of the boreholes by borehole camera. The different rock units identified in the project area include Iskere Gneisses, Shengus Gneisses, Kamila Amphibolites, Kohistan Batholiths, and Superficial Deposits. The superficial deposits cover the valley slopes of the Indus River and its tributaries. They consist mainly of moraine deposits, glaciofluvial deposits, talus cone/scree and landslide materials. The Iskere Gneiss and Amphibolite are the major geological units along the headrace tunnels route. Through geological mapping along the Headrace tunnels alignment, the tunnels pass through Iskere Gneisses towards the Intake area and amphibolite towards the Powerhouse area.

The bedrock information from the borehole at the Intake area has been considered in the assessment of the conditions at the dam site. Similarly, the

information from the boreholes at the Surge shaft has been considered in the assessment of the conditions at the Powerhouse. In terms of assessing the ground conditions along HRT, it is considered that the ground conditions at the Powerhouse can be assumed for the section of tunnel within the Kamila Amphibolite. Similarly, in assessing the ground conditions along HRT, it is considered that the ground condition at the dam site can be assumed for the section of the tunnel within the Iskere Gneisses. The two rock units are separated by the main mantle thrust (MMT) fault zone. Rock mass properties, groundwater conditions, and in-situ stress conditions have not been confirmed at the headrace tunnel elevation. Further, this work is limited to the two major rock units along the headrace tunnel and does not cover the shear zone of MMT.

The Iskere gneisses are comprised of quartz, feldspar, and biotite. Biotite commonly occurs in the form of banding, with a thickness of 50 to 200 mm. Mylonisation such as augen gneiss are very common in the gneisses. Generally, the rocks are slightly to highly jointed, locally massive, and slightly to moderately weathered. The main joint set is the foliation joints, and most joints including other tectonic origins have been re-cemented with secondary minerals such as calcite and quartzite. The borehole logs indicate that there are three typical discontinuity sets that are typically rough, planar or undulating with an aperture usually less than 1mm and with an infilling of calcite. The discontinuity characteristics are shown in Table 1. Discontinuity D_1 and D_2 are common sets of discontinuities; however, they are either augmented with D_3 or D_4 at the dam site.

Table 1. Discontinuity characteristics at dam and power house.

Set number	Dip (°)	Dip direction (°)
D_1	44	220
D_2	75	251
D_3	56	350
D_4	54	110
P_1	70	250
P_2	30	074
P_3	70	160
P_4	65	335

The amphibolite rocks are fine-grained and very micaceous, with quartz veins at places. These rocks are generally slightly weathered and slightly to moderately fractured at outcrop but are very hard. At the powerhouse area, the analysis of the orientation of discontinuity sets P_1, P_2, and P_3/P_4 indicate that they comprise a system of mutually orthogonal joints, and therefore, should lead to a blocky rock mass. These discontinuities are mostly undulating or stepped rough, although there is a significant number described as planar rough. The majority of discontinuities at outcrop are described as having an aperture less than 1mm and infilled with swelling clay. The investigations show P_1 and P_2 almost everywhere, but at some location, P_3 and P_4, are also available.

Along with the field investigation, a comprehensive laboratory testing programme has been undertaken. Based on the laboratory tests results, the physical and geomechanical properties of the Iskere Gneisses and Amphibolite are given in Table 2. These results are based on the reports of the pre-feasibility, feasibility and detail design stage. The average test results are used in this study.

Table 2. Rock test results of Iskere Gneisses and Amphibolite rock units.

Type of tests	Iskere Gneiss					Kamila Amphibolite				
	No.s of tests	Min.	Max	Mean	Average	Nos of tests	Min.	Max	Mean	Average
Density (Mg/m^3)	644	2.12	3.06	2.73	2.74	256	2.12	3.36	2.84	2.82
UCS (MPa)	404	8	201	49	50.7	132	13.2	125.8	56.5	61
Point load index (MPa)	2189	0.09	35.44	3.61	3.91	394	0.48	13.42	4.12	4.50
BTS (MPa)	95	1.89	16.72	8.89	8.62	27	3.5	12.9	9.02	8.56
E (GPa)	238	4.02	109	16.5	20.81	75	2.4	95	24.8	27.4
Poison's ratio	238	0.012	0.78	0.123	0.173	75	0.018	0.593	0.11	0.179

3.1. Rock mass classification systems and tunnel support

3.1.1. RMR

The RMR system was developed in 1973 from the experience of tunnel projects, and refined over the years as the tunnelling data pool enriched [10, 35]. The six-parameter RMR_{89} is still used in the field, although the eight parameter RMR_{14} version was proposed with a modified rating structure [13], as given by Equation 1.

$$RMR_{14} = (RMR_b + F_0) \times F_s \times F_e \quad (1)$$

where RMR_b is basic RMR, F_0 is the joint orientation parameter, F_s parameter predicts the stress-strain behavior at excavation faces, and F_e is the parameter related to the excavation method.

Though the RMR system is improved massively in terms of characterization, its application in high-stress environments remains its limitation in deep tunnel design [36]. Through hypothesis, stress adjustment factors are recommended in 2019 for RMR_{89} and RMR_{14} to extend their application to stress environments [8], as given by Equations 2 and 3.

$$RMR_{19} = RMR_{89} + F_{stress\text{-}89} \quad (2)$$

$$RMR_{19} = RMR_{14} + F_{stress\text{-}14} \quad (3)$$

where $F_{stress\text{-}89}$ and $F_{stress\text{-}14}$ are the stress adjustment factors for RMR_{89} and RMR_{14}, respectively. The rating of these parameters, based on the strength-stress ratio, is given in Table 3.

Table 3. Stress adjustment factors for two versions of RMR.

Stress adjustment factor	Values of σ_c/σ_1		
	5-4	4-3	3-2
$F_{stress\text{-}89}$	-5	-10	-15
$F_{stress\text{-}14}$	-22.326	-27.169	-32.012

3.1.2. Q-system

1n 1974, the tunneling data-based Q system was presented for rock mass classification and tunnel support design and refined with time [11, 14], which can be determined from Equations 4 and 5. In the rock-mass properties, the role of intact rock UCS (uniaxial compressive strength) is significant. Thus a normalization factor is applied to Equation 4 for a modified Q_c:

$$Q = \left(\frac{RQD}{J_n}\right).\left(\frac{J_r}{J_a}\right).\left(\frac{J_w}{SRF}\right) \quad (4)$$

$$Q_c = \left(\frac{RQD}{J_n}\right).\left(\frac{J_r}{J_a}\right).\left(\frac{J_w}{SRF}\right).\left(\frac{\sigma_c}{100}\right) \quad (5)$$

where RQD is rock quality designation, J_n symbolizes the rating of the number of joint sets, J_r is the rating for the joint surface roughness, J_a denotes the rating for the degree of alteration or clay filling joint set, J_w denotes the ratings for groundwater inflow and pressure effects, and the stress reduction factor (SRF) is the rating for faulting, strength– stress ratios in hard rocks, and squeezing or swelling. To adopt this tunnelling data-based Q-system in the mining sector of South Africa, Equation 6 was suggested for the SRF characterization [37]:

$$SRF = 0.244 \times K^{0.346} \times \left(\frac{H}{\sigma_c}\right)^{1.322} + 0.176 \times \left(\frac{\sigma_c}{H}\right)^{1.413} \quad (6)$$

In Equation 6, H is the overburden height in m and K is the stress ratio. Taking the average density of Iskere Gneiss and Kamila Amphibolite (Table 2), Equation 6 can be re-written as 7 and 8, respectively.

$$SRF = 29.1 \times \left(\frac{\sigma_1}{\sigma_3}\right)^{0.346} \times \left(\frac{\sigma_c}{\sigma_1}\right)^{-1.322} + 0.00106 \times \left(\frac{\sigma_c}{\sigma_1}\right)^{1.413} \quad (7)$$

$$SRF = 28.0 \times \left(\frac{\sigma_1}{\sigma_3}\right)^{0.346} \times \left(\frac{\sigma_c}{\sigma_1}\right)^{-1.322} + 0.0011 \times \left(\frac{\sigma_c}{\sigma_1}\right)^{1.413} \quad (8)$$

To characterize SRF for the Australian mining field, Equation (9) was proposed [38].

$$SRF = 31 \times \left(\frac{\sigma_1}{\sigma_3}\right)^{0.3} \times \left(\frac{\sigma_c}{\sigma_1}\right)^{-1.2} \quad (9)$$

From tunnel face characterization, installed support, and support chart of Q-system, new empirical equations (Equations 10 and 11) were empirically derived for SRF characterization in fractured rock mass under a high-stress environment [8, 17]. These two equations are based on the same data but give different weightage to rock bolt and shotcrete in the support during the back calculation.

$$SRF=2.0\exp\left(0.21\times\frac{RQD}{J_n}\right)+12.0\exp\left(-\alpha\times\frac{\sigma_c}{\sigma_1}\right) \quad (10)$$

$$SRF=2.054\exp\left(0.205\frac{RQD}{J_n}\right)+14.865\exp\left(-0.41\frac{\sigma_c}{\sigma_1}\right) \quad (11)$$

In Equation 10, the rating of constant α depends on the strength-stress ratio. From the exploration reports of the BHP, the two rock units were characterized and classified. RMR_{89}, RMR_{14}, and RMR_{19} were determined, and the details are shown in Tables 4 and 5. According to Table 4, the RMR_{89} values are 60.86 and 63.1 for Iskere Gneiss and Amphibolite rock units, respectively. With the application of the stress adjustment factor according to Table 3 guidelines, the RMR_{19} values are 55.86 and 53.1 for the two rock units, respectively.

Table 4. Characterization and classification of two rock units, based on RMR_{89} and RMR_{19}.

Classification parameters		Value (rating)	
		Amphibolite	Iskere Gneiss
UCS (Mpa)		61 (6.2)	50.7 (5.36)
RQD (%)		90 (18.2)	85 (17.26)
Spacing (m)		0.85 (14.7)	0.4 (11.24)
Discontinuities condition	Persistence (m)	3–10 (2)	3–10 (2)
	Aperture (mm)	1 (4)	1 (4)
	Weathering	Slightly (5)	No weathering (6)
	Roughness	Stepped rough and undulating rough (6)	Undulating rough (6)
	Infilling	Soft (2)	Calcite (4)
Groundwater conditions		Dry (15)	Dry (15)
RMR_b		73.1	70.86
Discontinuities orientation		-10	-10
RMR_{89}		63.1	60.86
Strength stress ratio		3.5 (-10)	4.5 (-5)
RMR_{19}		53.1	55.86

According to Table 5, the RMR_{14} values are 72.88 and 78.04 for Iskere Gneiss and Amphibolite rock units, respectively. With the application of the stress adjustment factor according to Table 3 guidelines, the RMR_{19} values are 50.55 and 50.88 for the two rock units, respectively. In Table 5, ICE is Índice de Comportamiento Elástico (Spanish), and defines the elastic behaviour index [39].

SRF was characterized using the previous Equations 6-11 for the two rock units, and the corresponding Q-values were calculated. The rock mass qualities, using the different SRF characterization, for Amphibolite and Iskere Gneiss are summarized in Table 6. Equations 7 and 8, which are the extensions of Equation 6, give 4 and 5.35 SRF values and the corresponding 7.08 and 5.61 Q-values for the Iskere Gneiss and Amphibolite rock units respectively. According to Equation 9, the SRF values are 5.1 and 6.9, and the corresponding Q values are 5.56 and 4.35 for the two rock units, respectively. According to Equations 10 and 11, the SRF values are 16.57 and 19.49 for the two rock units, and the corresponding Q values are 1.71 and 1.54, respectively.

Table 5. Characterization and classification of two rock units based on RMR_{14} and RMR_{19}.

Classification parameters		Value (*rating*)	
		Amphibolite	**Iskere Gneiss**
Joints per meter		3.5 (29.3)	7.5 (24.4)
UCS (Mpa)		61 (6.2)	50.7 (5.36)
Discontinuities condition	Infilling	Soft (2)	Calcite (5)
	Weathering	Slightly (5)	No weathering (5)
	Persistence (m)	3-10 (2)	3-10 (2)
	Roughness	Stepped rough and undulating rough (5)	Undulating rough (5)
Groundwater conditions		Dry (15)	Dry (15)
Alterability		> 85% (10)	> 85% (10)
RMR_b		74.5	71.76
Adjustment factor	F_0	-10	-10
	F_e	1	1
	ICE	38.54	43.77
	F_s	1.21	1.18
RMR_{14}		78.045	72.88
Strength stress ratio		3.5 (-27.169)	4.5 (-22.326)
RMR_{19}		50.88	50.55

Table 6. Characterization and classification of two rock units based on Q-system, considering SRF calculation using different.

Classification parameters		Value (*Rating*)	
		Amphibolite	**Iskere Gneiss**
RQD (%)		90% (*90*)	85% (*85*)
Joint alteration number (J_r)		Rough, undulating (*3*)	Rough, undulating (*3*)
Joint alteration number (J_a)		Unaltered, surface staining only (*1*)	Unaltered, surface staining only (*1*)
Joint set number (J_n)		3 joints sets (*9*)	3 joints sets (*9*)
Joint water reduction factor (J_w)		Dry condition (*1*)	Dry condition (*1*)
Intact rock strength (σ_c) MPa		61 (61)	50.7 (50.7)
SRF	Equations 6-8	5.35 (5.35)	4.0 (4)
	Equation 9	6.9 (6.9)	5.1 (5.1)
	Equations 10-11	19.49 (19.49)	16.57 (16.57)
Q based on Equations 6-8		5.61	7.08
Q based on Equation 9		4.35	5.56
Q based on Equations 10-11		1.54	1.71

Considering the rock mass quality (Tables 4–6), tunnel supports were determined from the support charts and Equations [40, 41], as explained in Table 7. The SRF values were determined from Equations 10 and 11 and the corresponding determined Q values along with RMR_{19} suggest heavy supports in terms of rock bolts and shotcrete. In summary, the modified versions of RMR and Q-systems (RMR_{19} and Equations 10 and 11 based Q system) suggest 4 m rock bolts with 1.7-1.8 m spacing and 9 to 10 cm thick shotcrete. The remaining versions of the RMR and Q system (previous studies) suggest 3-4 m rock bolts with 2.2 m spacing and an average of 6 cm thick shotcrete.

3.2. Numerical Modelling

FLAC is a suited geotechnical modelling program for sequential excavation. The 7.0 explicit version 2D finite difference FLAC program is used in this work. The construction sequence of the headrace tunnel is divided into two major excavation stages (as shown in Figure 2):

1. *Top-heading excavation*
2. *Bench excavation*

Each excavation stage is accomplished in three construction steps:

1. *Initial excavation*
2. *Spraying of soft shotcrete and installation of rockbolt support*
3. *Shotcrete hardening*

Table 7. Support comparison obtained from different versions of RMR and different SRF characterization equations.

Classification system		Iskere Gneiss		Amphibolite	
		Shotcrete thickness (cm)	Rock bolt spacing (m) and length (m)	Shotcrete thickness (cm)	Rock bolt spacing (m) and length (m)
Original	RMR_{89}	8	2.1 and 3	7	2.2 and 3
	RMR_{14}	5	2.5 and 3	3	2.7 and 3
Modified for stress factor	RMR_{19}	10	1.8 and 4	10	1.8 and 4
Based on Equation 6-8 (original)	Q	5-6	2.2 and 3-4	5-6	2.2 and 3-4
Based on Equation 9 (original)		5-6	2.2 and 3-4	6	2.1 and 3-4
Based on Equation 10-11 (modified)		9	1.7-1.8 and 3-4	9	1.7-1.8 and 3-4

The displacement and stress fields during tunnel construction change in the advancing direction and are most thoroughly analyzed via a three-dimensional program. However, the excavation problems in the case of tunnels are frequently assessed in 2D modelling by ignoring displacements perpendicular to the cross-section of tunnel. Adequate distances were kept between the boundaries and tunnel periphery to avoid the boundary effect. The 80 m × 60 m model dimensions and modified Hoek-Brown model was used in the numerical model. In the tunnel vicinity, the fine mesh was applied to obtain better results. The modified Hoek-Brown model adopts a non-linear relation between minor (σ_3) and major principal (σ_1) stresses. The model was fixed at all sides except at the top, where σ_{yy} (vertical stresses) were applied. Besides σ_{yy}, the gravity, and FISH function were used to create an in-situ stress environment. The model is brought to an initial force-equilibrium state under gravitational loading. The empirically suggested supports shown in Table 7 are used in the models. The rockbolts and shotcrete are modelled and simulated via rockbolt elements and elastic liner elements, respectively. To limit the number of cases for numerical modelling, two sets of supports were used; i. 4 m rock bolts having 1.75 m spacing with 10 cm thick shotcrete, and ii. 3 m rock bolts having 2.2 m spacing and 6 cm thick shotcrete. The axial forces in the rockbolts and shotcrete are compared for the two support pattern at 100 percent relaxation.

3.3. Intact rock and rock mass properties

The adopted failure criterion (generalized Hoek-Brown) [31] is a well-recognised method for measuring the mechanical properties of rock masses. The average intact rock properties of the two rock units were converted to the rock mass with the help of RocLab software, which is based on the aforementioned criteria, as displayed in Table 8. The typical GSI values have been derived from the results of the boreholes and the scanlines, both at dam and powerhouse sites. At the dam site, the GSI values range from 46 to 77 with an average value of 61. Similarly, at the powerhouse site, these values are from 50 to 79 with an average value of 67. Comparing these GSI values with the RMR_{89} and RMR_{14} values, the results show that the quality of Amphibolte rock is comparatively higher than Iskere Gneiss. As the core target of this work is to numerically assess empirically derived SRF characterization equation and RMR_{19}, therefore, 420 and 630 m overburden is used in this work for the Iskere Gneiss and Amphibolite rock units to create the 4.5 and 3.5 cases of σ_c/σ_1 ratio.

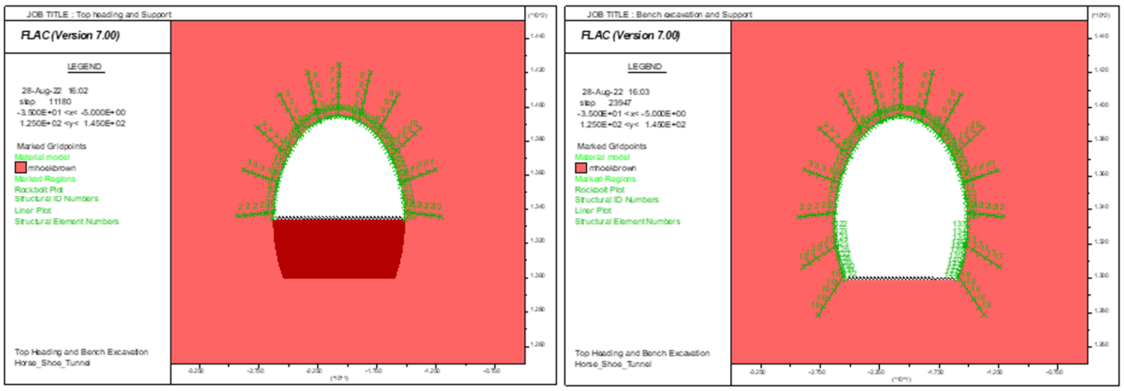

a) Original tunnel support

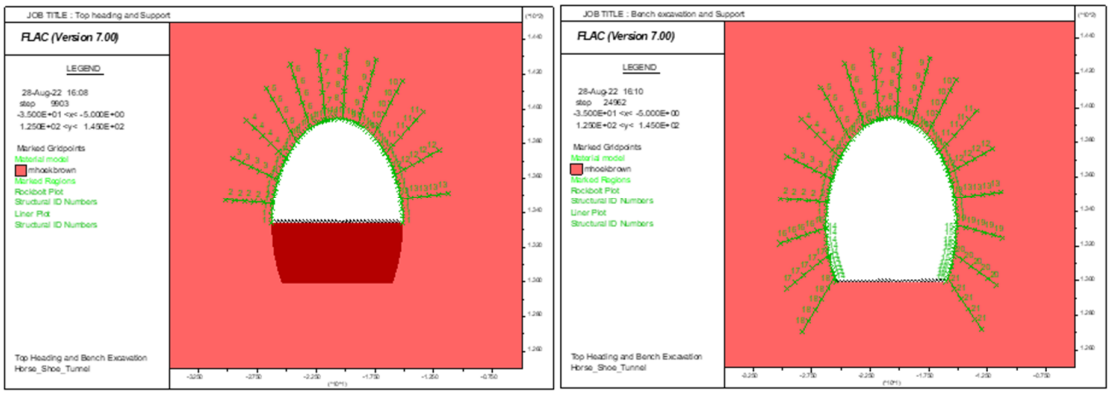

b) Modified tunnel support

Figure 2. Two excavation stages (top heading (left) and bench (right)) with support pattern.

Table 8. Rock mass properties for two rock units.

Rock types	*GSI*	*mi*	*c* (MPa)	*Φ* (°)	m_b	*a*	*s*	Sigt (MPa)	Sigc (MPa)	E_{rm} (GPa)
Iskere gneiss	61	28	2.265	49.59	6.954	0.503	0.0131	-0.096	5.742	11.294
Amphibolite	67	26	3.447	48.74	8.0	0.502	0.0256	-0.195	9.692	18.466

4. Results and Discussion

The FLAC 2D model is solved for the Iskere gneiss and Amphibolite rock units, separately for the original and modified supports. The results from modelling are compared and evaluated in terms of axial forces (rock bolts), stability of liner, and stress variable (e). The bolts numbering is changed in the two cases due to the sequence in which these bolts are installed in the model. For liner stability, graphical capacity diagrams [42] are used. In tunnelling, the variation of σ_1 and σ_3 from the tunnel periphery is shown in Figure 3 [43]. σ_3 was gradually increased from zero with the distance from the tunnel boundary. On the other hand, σ_1 was at its peak at periphery and gradually decreased with the distance. The "e" is defined in Equation 12 [44] as the ratio of the difference between σ_1 (σ_{max}) and σ_3 (σ_{min}) the to the σ_1. In tunnelling, the rock load is defined as the area that starts from the peak principal stress around the tunnel periphery and ends at the point where the "e" is achieved as 10% [29, 44, 45]. Around the tunnel, radial (σ_r) and tangential stresses (σ_θ) are the minimum (σ_{min}) and maximum (σ_{max}) principal stresses, respectively.

$$e\ (\%) = \frac{\sigma_{max} - \sigma_{min}}{\sigma_{max}} \times 100 \qquad (12)$$

As it can be perceived in Figure 4, bolts in the original tunnel supports are experiencing high axial stresses when compared with the modified tunnel support rock bolts. The highest axial stresses in the original tunnel support are 1.382E05 and 1.180E05 for the amphibolite and Iskere Gneiss rock units, respectively (Figure 4a). These maximum stresses are 1.006E05 and 1.065E05, respectively, for the two rock units in case of modified tunnel support (Figure 4b). Relating the axial stresses, the bolts pattern in the amphibolite rock are relatively more

loaded than the Iskere Gneiss rock. Although the rock mass properties of amphibolite are superior than the Iskere Gneiss, however the in-situ stresses are higher in the case of amphibolite. The low axial stress in the modified tunnel support case reveals that rock bolts are much safer in this case.

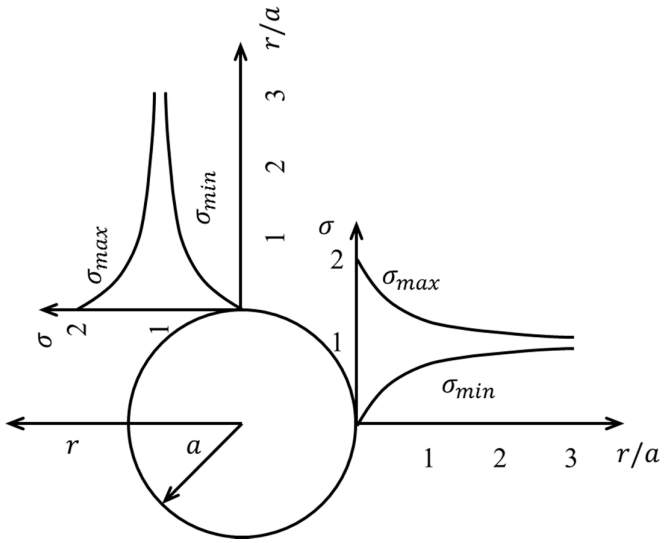

Figure 3. Variation of principal stresses around underground excavation.

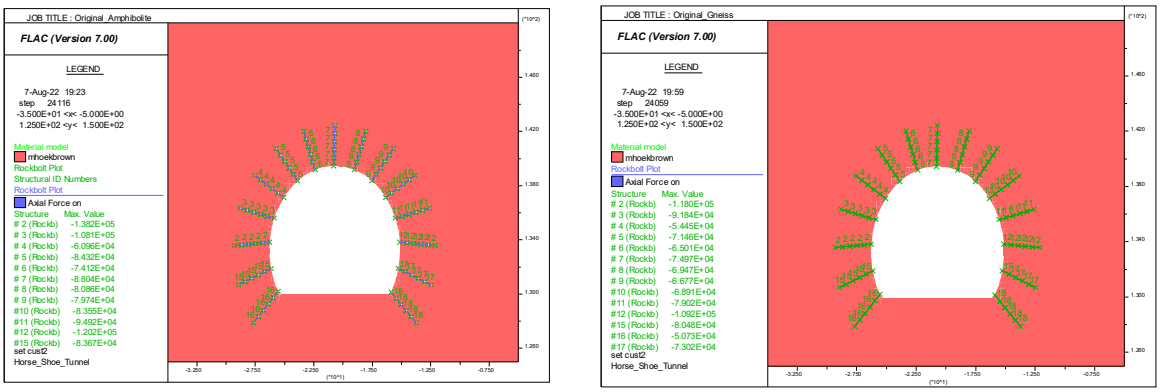

a) Original tunnel support

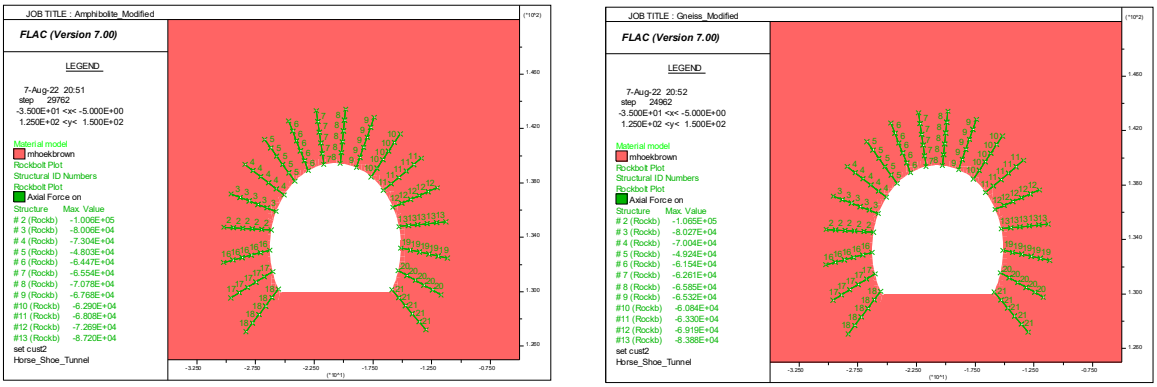

b) Modified tunnel support

Figure 4. Axial stresses on bolts in different rock units (Amphibolite (left) and Iskere Gneiss (right)).

Capacity diagrams reveal the relations of thrust-shear forces and thrust-bending moments and to evaluate the liner stability. Based on the proposed thickness of shotcrete, the induced axial thrust and

bending moment on a liner plotted together with the corresponding envelop of failure for the different factors of safety (FOS) of 1.5, 2.0, and 2.5, respectively, as shown in Figure 5. The plotted thrust-bending moment interaction diagrams are shown in the figure below for 6 and 10 cm thick shotcrete/liner. The utility command function of the model was used for the liner information. The thrust bending moment for the liner shows that for the original support, the main instability type was in compression for the original support and too many points show a FOS < 02. However, after the installation of modified support, only the corner nodes face a low factor of safety due to stress concentration in the corners and the majority of nodes show a FOS > 02.

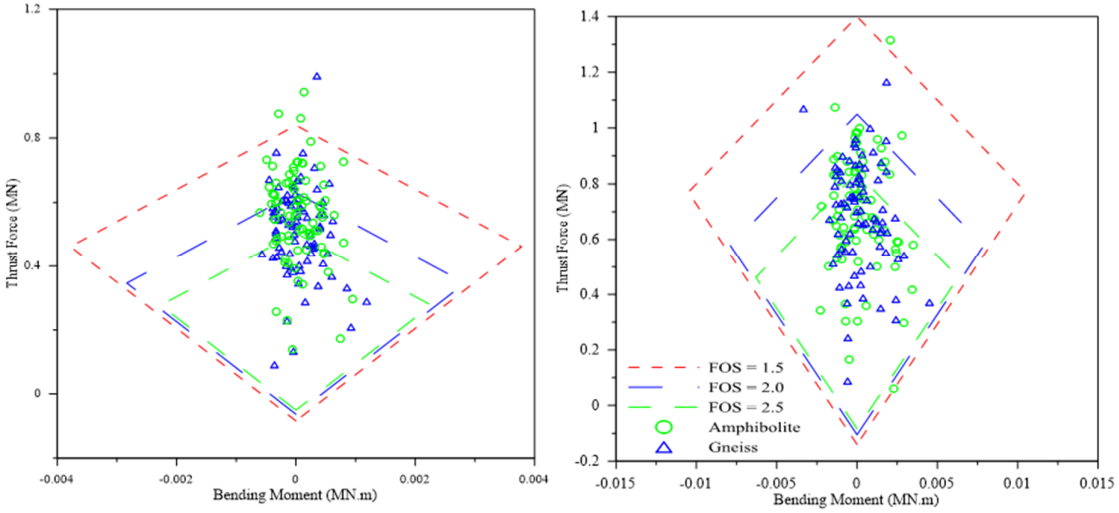

a) 6 cm thick shotcrete **b). 10 cm thick shotcrete**

Figure 5. Thrust-Bending moment diagram of shotcrete/liner for different FOSs.

The FISH functions were used to extract e contours for two rock units and two different supports. In the case of original support, the thickness of the rock load area is 3.7 m for both the amphibolite and Iskere Gneiss rock units. The e contour for the amphibolite rock unit with original support is shown in Figure 6. However, this thickness was reduced by 0.1 m with modified support. The role of support is to provide the confining stress and as a result, increase the radial stress. This increase in radial stress decreases the thickness of the rock load area.

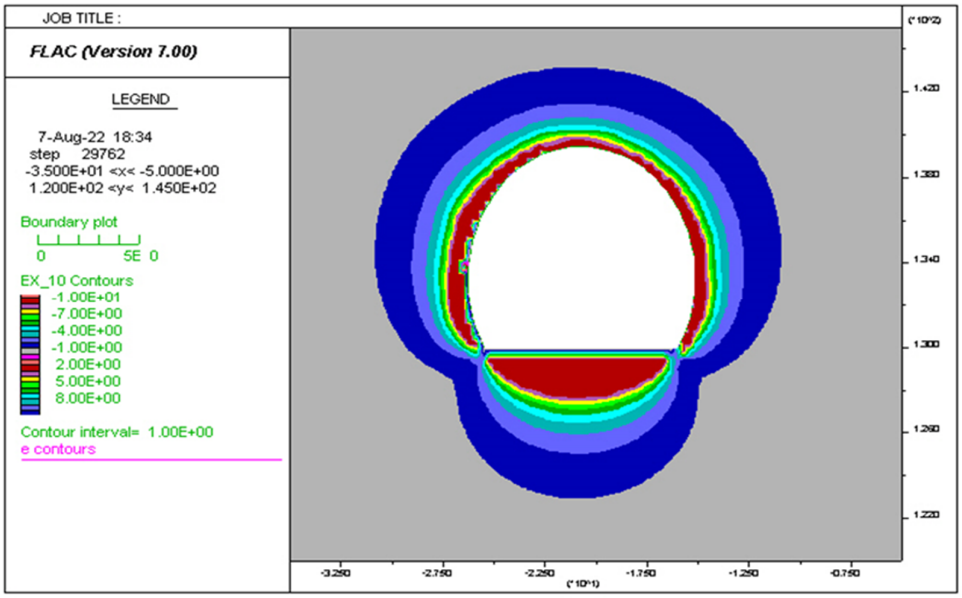

Figure 6. Rock load evaluation based on stress transfer effect.

5. Conclusions

In this work, the modified versions of RMR and Q-system were adopted for the rock mass characterization along the typical horse-shoe-shaped headrace tunnel of the Bunji hydropower project. The tunnel support pattern was determined from the field information and laboratory test results. The support pattern was obtained from the modified version, and the previous studies were analysed through finite difference modelling. The modelling results were compared in terms of axial stresses in rock bolts, liner stability through the capacity diagram, and rock load through the stress transfer effect. The following conclusions are obtained from this work:

1. The latest version of the two systems considered heavier support in the two highly stressed jointed rock mass units along the headrace tunnel in term of shotcrete thickness and bolts.
2. The modelling results in terms of axial forces on rock bolts revealed that bolts installed as per the latest version experienced a lower amount of stress. These stresses are 1.006E05 and 1.065E05, which are much lower than the axial stresses on the rock bolts, installed in the original tunnel support pattern.
3. Evaluation of the shotcrete through the capacity diagram confirms a high safety factor in the modified support pattern. From the comparison, the majority of shotcrete elements show higher FOS (> 2) as compared to the original support.
4. It is further verified that with the application of a modified support pattern, the thickness of the rock load area decreased by 0.1 m in the two rock units as compared to the original support pattern.

Thus, it can be assumed that the tunnel support pattern suggested by the modified version of RMR and Q-systems are more appropriate for highly stressed jointed rock masses.

References

[1]. Mirza, U.K., N. Ahmad, T. Majeed, and K. Harijan. (2008). Hydropower use in Pakistan: past, present and future. Renewable and Sustainable Energy Reviews, 12(6): p. 1641-1651.

[2]. Carter, T. (Year of conference). Himalayan Ground Conditions challenge innovation for successful TBM Tunnelling. in Invited paper in Proc. Hydrovision India 2011 Conf, Delhi. SESSION 5c:(Risk Management in Tunnelling), 20pp.

[3]. Panthi, K.K. (2012). Evaluation of rock bursting phenomena in a tunnel in the Himalayas. Bulletin of Engineering Geology and the Environment, 71(4): p. 761-769.

[4]. Palmstrom, A. and H. Stille. (2007). Ground behaviour and rock engineering tools for underground excavations. Tunnelling and Underground Space Technology, 22(4): p. 363-376.

[5]. Stille, H. and A. Palmström. (2008). Ground behaviour and rock mass composition in underground excavations. Tunnelling and Underground Space Technology, 23(1): p. 46-64.

[6]. Sharma, H. and A. Tiwari. (2012). Tunnelling in the Himalayan Region: geological problems and solutions. International Water Power and Dam Construction, 64(9): p. 14-19.

[7]. Rehman, H., A.M. Naji, K. Nam, S. Ahmad, K. Muhammad, and H.-K. Yoo. (2021). Impact of construction method and ground composition on headrace tunnel stability in the Neelum–Jhelum Hydroelectric Project: A case study review from Pakistan. Applied Sciences, 11(4): p. 1655.

[8]. Rehman, H., A.M. Naji, J.-j. Kim, and H. Yoo. (2019). Extension of tunneling quality index and rock mass rating systems for tunnel support design through back calculations in highly stressed jointed rock mass: An empirical approach based on tunneling data from Himalaya. Tunnelling and Underground Space Technology, 85: p. 29-42.

[9]. Hoek, E. (2001). Big tunnels in bad rock. Journal of Geotechnical and Geoenvironmental Engineering, 127(9): p. 726-740.

[10]. Rehman, H., W. Ali, A. Naji, J.-j. Kim, R. Abdullah, and H.-k. Yoo. (2018). Review of Rock-Mass Rating and Tunneling Quality Index Systems for Tunnel Design: Development, Refinement, Application and Limitation. Applied Sciences, 8(8): p. 1250.

[11]. Barton, N., R. Lien, and J. Lunde. (1974). Engineering classification of rock masses for the design of tunnel support. Rock mechanics, 6(4): p. 189-236.

[12]. Bieniawski, Z.T., Engineering rock mass classifications: a complete manual for engineers and geologists in mining, civil, and petroleum engineering. 1989: John Wiley & Sons.

[13]. Celada, B., I. Tardáguila, P. Varona, A. Rodríguez, and Z. Bieniawski. (Year of conference). Innovating tunnel design by an improved experience-based RMR system. in World Tunnel Congress. Proceedings… Foz do Iguaçu, Brazil.

[14]. Barton, N. (2002). Some new Q-value correlations to assist in site characterisation and tunnel design. International journal of rock mechanics and mining sciences, 39(2): p. 185-216.

[15]. Marinos, P. and E. Hoek. (Year of conference). GSI: a geologically friendly tool for rock mass strength estimation. in ISRM international symposium. OnePetro.

[16]. Rehman, H., J.-J. Kim, and H.-K. Yoo. (Year of conference). Stress reduction factor characterization for

highly stressed jointed rock based on tunneling data from Pakistan. in World Congress on Advances in Structural Engineering and Mechanics (ASEM17). Seoul, Korea.

[17]. Lee, J., H. Rehman, A. Naji, J.-J. Kim, and H.-K. Yoo. (2018). An Empirical Approach for Tunnel Support Design through Q and RMi Systems in Fractured Rock Mass. Applied Sciences, 8(12): p. 2659.

[18]. Pinheiro, M., X. Emery, T. Miranda, L. Lamas, and M. Espada. (2018). Modelling Geotechnical Heterogeneities Using Geostatistical Simulation and Finite Differences Analysis. Minerals, 8(2): p. 52.

[19]. Feng, X.-T. and J.A. Hudson, Rock engineering design. 2011: CRC Press.

[20]. Lak, M., M. Fatehi Marji, A. Yarahamdi Bafghi, and A. Abdollahipour. (2019). Discrete element modeling of explosion-induced fracture extension in jointed rock masses. Journal of Mining and Environment, 10(1): p. 125-138.

[21]. Zhou, F., V. Sarfarazi, H. Haeri, M.H. Soleymanipargoo, J. Fu, and M.F. Marji. (2021). A coupled experimental and numerical simulation of concrete joints' behaviors in tunnel support using concrete specimens. Computers and Concrete, 28(2): p. 189-208.

[22]. Haeri, H., V. Sarfarazi, P. Ebneabbasi, A. Shahbazian, M.F. Marji, and A. Mohamadi. (2020). XFEM and experimental simulation of failure mechanism of non-persistent joints in mortar under compression. Construction and Building Materials, 236: p. 117500.

[23]. Manouchehrian, A., M.F. Marji, and M. Mohebbi. (2012). Comparison of indirect boundary element and finite element methods. Frontiers of Structural and Civil Engineering, 6(4): p. 385-392.

[24]. Lak, M., M.F. Marji, A.Y. Bafghi, and A. Abdollahipour. (2019). A coupled finite difference-boundary element method for modeling the propagation of explosion-induced radial cracks around a wellbore. Journal of Natural Gas Science and Engineering, 64: p. 41-51.

[25]. Abdollahi, M.S., M. Najafi, A.Y. Bafghi, and M.F. Marji. (2019). A 3D numerical model to determine suitable reinforcement strategies for passing TBM through a fault zone, a case study: Safaroud water transmission tunnel, Iran. Tunnelling and Underground Space Technology, 88: p. 186-199.

[26]. Ali, W., H. Rehman, R. Abdullah, Q. Xie, and Y. Ban. (2022). TOPOGRAPHY INDUCED STRESS AND ITS INFLUENCE ON TUNNEL EXCAVATION IN HARD ROCKS–A NUMERICAL APPROACH. GEOMATE Journal, 22(94): p. 93-101.

[27]. Nikadat, N. and M.F. Marji. (2016). Analysis of stress distribution around tunnels by hybridized FSM and DDM considering the influences of joints parameters. Geomechanics & engineering, 11(2): p. 269-288.

[28]. Nikadat, N., M. Fatehi, and A. Abdollahipour. (2015). Numerical modelling of stress analysis around rectangular tunnels with large discontinuities (fault) by a hybridized indirect BEM. Journal of Central South University, 22(11): p. 4291-4299.

[29]. Lee, J.-K., J. Kim, H. Rehman, and H.-K. Yoo, Evaluation of rock load based on stress transfer effect due to tunnel excavation. 2017.

[30]. Rehman, H., A.M. Naji, W. Ali, M. Junaid, R.A. Abdullah, and H.-k. Yoo. (2020). Numerical evaluation of new Austrian tunneling method excavation sequences: A case study. International Journal of Mining Science and Technology.

[31]. Hoek, E., C. Carranza-Torres, and B. Corkum. (2002). Hoek-Brown failure criterion-2002 edition. Proceedings of NARMS-Tac, 1: p. 267-273.

[32]. Bunji_Consultants, Main Report, Bunji Hydropower project. 2012.

[33]. Vestad, M. (2014). Analysis of the Deformation Behavior at the Underground Caverns of Neelum Jhelum HPP. Pakistan, Department of Geology and Mineral Resources Engineering, Norvegian University of Science and Technology.

[34]. DiPietro, J.A. and K.R. Pogue. (2004). Tectonostratigraphic subdivisions of the Himalaya: A view from the west. Tectonics, 23(5).

[35]. Bieniawski, Z. (1973). Engineering classification of jointed rock masses. Civil Engineer in South Africa, 15 (12): p. 333-343.

[36]. Rehman, H., A. Naji, J.-j. Kim, and H.-K. Yoo. (2018). Empirical Evaluation of Rock Mass Rating and Tunneling Quality Index System for Tunnel Support Design. Applied Sciences, 8(5): p. 782.

[37]. Kirsten, H., Case histories of groundmass characterization for excavatability, in Rock classification systems for engineering purposes. 1988, ASTM International.

[38]. Peck, W. (2000). Determining the stress reduction factor in highly stressed jointed rock. Aust Geomech, 35(2).

[39]. BIENIAWSKI, R.Z., D. AGUADO, B. CELADA, and A. RODRIQUEZ. (2011). Forecasting tunnelling behaviour. T & T international, (AOU): p. 39-42.

[40]. NGI. The Q-system, Rock mass classification and support design. 2015 09 04 2018]; Available from: https://www.ngi.no/eng/Publications-and-library/Books/Q-system.

[41]. Lowson, A. and Z. Bieniawski. (Year of conference). Critical assessment of RMR based tunnel design practices: a practical engineer's approach. in

Proceedings of the SME, Rapid Excavation and Tunnelling Conference, Washington, DC.

[42]. Carranza-Torres, C. and M. Diederichs. (2009). Mechanical analysis of circular liners with particular reference to composite supports. For example, liners consisting of shotcrete and steel sets. Tunnelling and Underground Space Technology, 24(5): p. 506-532.

[43]. Lee, J.K., H. Yoo, H. Ban, and W.-J. Park. (2020). Estimation of rock load of multi-arch tunnel with cracks using stress variable method. Applied Sciences, 10(9): p. 3285.

[44]. Yang, J., S. Wang, Y. Wang, and C. Li. (2015). Analysis of arching mechanism and evolution characteristics of tunnel pressure arch. Jordan Journal of Civil Engineering, 9(1).

[45]. Wang, S.-r., C.-l. Li, Y.-g. Wang, and Z.-s. Zou. (2016). Evolution characteristics analysis of pressure-arch in a double-arch tunnel/Analiza razvoja znacajki tlacnog svoda u tunelu s dvostrukim svodom. Tehnicki Vjesnik-Technical Gazette, 23(1): p. 181-190.

تجزیه و تحلیل تفاضل محدود طراحی تجربی سیستم نگهداری تونل در محیط توده سنگ شکسته شده با تنش بالا در پروژه برق آبی Bunji، پاکستان

حافظ الرحمن[۱،۲]، وحید علی[۱]، کوثر سلطان شاه[۳]، مهد حزیزان بن محد هاشم[۲*]، ناصر محمد خان[۴]، محمدعلی[۱]، محمد کامران[۵]، و محمد جنید[۳]

۱. گروه مهندسی معدن، دانشگاه بلوچستان فناوری اطلاعات مهندسی و علوم مدیریت، کویته، پاکستان
۲. دانشکده مهندسی مواد و منابع معدنی، دانشگاه Sains مالزی، پردیس مهندسی، Nibong Tebal، پنانگ، مالزی
۳. گروه مهندسی معدن، دانشگاه بین المللی قراقورام، گیلگیت، پاکستان
۴. گروه مهندسی ژئومکانیک پیشرفته پایدار، دانشکده مهندسی نظامی، دانشگاه ملی علوم و فناوری، ریسالپور، پاکستان
۵. گروه مهندسی معدن، موسسه فناوری باندونگ، اندونزی

ارسال ۲۰۲۲/۰۸/۲۲، پذیرش ۲۰۲۲/۰۹/۰۲

* نویسنده مسئول مکاتبات: mohd_hazizan@usm.my

چکیده:

طراحی نگهدارنده هدف اصلی سیستم‌های رتبه بندی Q و توده سنگ (RMR) است. ارزیابی کاربرد سیستم Q و RMR در تونل‌زنی که شامل شرایط زمین با تنش بالا است نشان می‌دهد که سیستم اول به دلیل ضریب کاهش تنش مناسب‌تر است. اخیراً، این دو سیستم برای طراحی الگوی سیستم نگهداری حفاری در شرایط توده سنگی درزه‌ای و با تنش بالا به‌طور تجربی اصلاح شده‌اند. این کار تحقیقاتی با هدف برجسته کردن اهمیت مدل‌سازی عددی، و ارزیابی عددی الکوی سیستم نگهداری پیشنهادی تجربی برای تونل‌زنی در چنین محیطی است. یک تونل معمولی به شکل نعل اسب در سایت پروژه برق آبی Bunji برای این کار انتخاب شده است. داده‌های مغزه‌گیری گمانه نشان می‌دهد که آمفیبولیت و ایسکره گنیس واحدهای اصلی توده سنگ در طول مسیر تونل هستند. ارزیابی سیستم نگهداری پیشنهادی بر اساس سیستم‌های تجربی اصلاح‌شده نشان می‌دهد که سیستم‌های نگهداری اصلاح‌شده سنگین را در مقایسه با سیستم‌های تجربی اصلی پیشنهاد می‌کنند. خواص توده سنگ بکر و وزن مخصوص سنگ به عنوان ورودی برای مدلسازی عددی استفاده شد. از مدل‌سازی عددی، تنش‌های محوری روی پیچ‌های سنگ، گشتاور خمشی رانش شاتکریت، و بار سنگ از سیستم‌های RMR و Q اصلاح‌شده با مطالعات قبلی مقایسه شده‌اند. نتایج به‌دست‌آمده نشان می‌دهد که سیستم نگهداری طراحی‌شده بر اساس یک نسخه اصلاح‌شده از سیستم‌های تجربی نتایج بهتری را از نظر پایداری تونل در شرایط توده سنگ شکسته‌شده با تنش بالا تولید می‌کند.

کلمات کلیدی: تنش های درجا مقدار بالا، سیستم نگهداری تونل، توده سنگ درزه‌دار، مدل سازی عددی، روش‌های تجربی.